Chemical and Process Engineering Research
ISSN 2224-7467 (Paper) ISSN 2225-0913 (Online)
Vol.31, 2015

Effect of Prandtl Number on Linear Stability of Mixed Convective Flow in a Vertical Porous Annulus: A LTNE Approach

Moumita Bhowmik* P. Bera
Department of Mathematics, Indian Institute of Technology, Roorkee, 247667, India
* E-mail of the corresponding author: moumita2886@gmail.com

Abstract
A comprehensive numerical study on linear stability of fully developed mixed convective flow in a vertical annulus filled with saturated porous medium is investigated. A local thermal non-equilibrium (LTNE) approach is considered. The flow is induced by external pressure gradient and buoyancy force. The non-Darcy Brinkman-Forchheimer extended model is considered. The governing equations are solved by spectral collocation method. Special attention is given to understand the effect of thermal non-equilibrium parameters: inter phase heat transfer coefficient (H) and porosity scaled thermal conductivity ratio (γ) on instability boundary of basic flow in (Pr, Ra) -plane. Stability results indicate that for high permeable porous media depending on Prandtl number, the flow is least stable under either first azimuthal mode or zero azimuthal modes. The stability criteria of basic flow decreases on increasing the Prandtl number. Increasing of H stabilizes the basic flow, whereas, increasing of γ destabilizes it.
Keywords: Porous media, mixed convection, linear stability, thermal non-equilibrium, non-Darcy model.

1. Introduction

Mixed convective flow in a vertical system filled with porous media is considered as one of the most important processes in many areas of science and engineering projects such as heat exchange, cooling of nuclear reactors during emergency shutdown, electronic equipment and other areas of practical interests. In most of the engineering processes, the fluid and solid phases are not in thermal equilibrium state i.e., the temperature between two phases are expected to be different from the same under local thermal equilibrium (LTE) approximation. In this situation separate energy equations need to be considered for solid and fluid phases. This situation is known as local thermal non-equilibrium (LTNE) state. Freezing/drying of foods (Zorrilla & Rubiolo 2005), computer chips via use of porous metal foams (Calmidi & Mahajan 2000) are important applications in porous media under LTNE condition. Therefore it is an important to study the flow dynamics as well as heat transfer mechanism in such environments. Linear stability plays a vital role in this study. It is concerned with when and how laminar flows break down, their subsequent development and their transition to turbulence. The aim of the linear stability is to find whether a given laminar flow is unstable and, if so, to find how it breaks down into turbulence or some other laminar flow. The rapid development of this theory in recent decades has resulted in huge number of studied in various fields such as petroleum industries, chemical technology and geophysical sciences etc. The growing volume of work in this area is amply documented in the review books Nield & Bejan (2013) and Vafai (2005).

A pioneer work on linear stability analysis in channel (Chen & Chung 1996; Chen 2000; Bera & Khalili 2002; Bera & Khalili 2006; Bera & Khalili 2007; Kumar *et al.* 2010), in pipe (Yao 1987a; Yao 1987b; Su & Chung 2000; Bera & Kumar 2011), in annulus (Rao & EL-Genk 1990; Yao & Rogers 1989a; Yao & Rogers 1989b; Rogers & Yao 1993) are focused on mixed convection in a wall bounded vertical system in pure viscous as well as porous media. Among these, a theoretical work on hydrodynamic stability of mixed convective flow in a vertical pipe is investigated by Yao (Yao 1987a; Yao 1987b). He has performed a linear stability analysis for heated pipe flow of water and found that the fully developed non-isothermal flow is highly unstable. He has also found that the first azimuthal mode is the least stable for all *Re*, except in the range [-50,150] of *Re*. Su & Chung (2000) have presented the linear stability of mixed convective flow in a vertical pipe for both cases buoyancy assisted and buoyancy opposed. They have mentioned that most unstable azimuthal wave is unity. Later on Rao & EL-Genk (1990) have reported some experimental results for buoyancy induced instability in a vertical annulus for low Reynolds number (*Re*) flows. Yao and his group (Yao & Rogers 1989a; Yao & Rogers 1989b; Rogers & Yao 1993) have also reported some important works on linear stability of mixed convective flow in vertical annulus with two different types of boundary conditions: (i) each cylinder is maintained at a different temperature, and (ii) vertical temperature gradient condition is imposed on the inner cylinder and outer cylinder is insulated. They have observed three distinct types of instability namely: shear, thermal shear and interactive instability under first type of boundary condition. However, under second type of boundary condition, they have found thermal instability and named as thermal-buoyant instability (Rogers & Yao 1993). The source of thermal-buoyant instability in kinetic energy spectrum is mainly from thermal buoyant potential, and it occurs for high Prandtl number fluids. Later on in case of buoyancy opposed flow, the Rayleigh Taylor instability is most dominant for $Pr \geq 100$. A linear stability analysis of non-isothermal poiseuille flow in a vertical channel is carried out by Chen & Chung (1996). They have found that the least stable mode is 2D. They have also reported that in buoyancy assisted case the types of instabilities are shear and thermal, whereas, in buoyancy opposed case the dominant stability is Rayleigh Taylor mode.

The above mentioned work is available in viscous media but substantial amount of the work on linear stability of mixed convective flow in porous media is also carried out by researchers (Bera & Khalili 2002; Bera & Khalili 2006; Bera & Khalili 2007; Kumar *et al.* 2010). Bera et al. have investigated the linear stability of the mixed convection in vertical channel filled with isotropic and anisotropic porous media under LTE state. They have found that a fully developed 1D flow does not remain 1D beyond the critical Ra. They have also found that types of instabilities are shear, thermal, mixed mode type. The least stable mode in porous media is also 2D. Later on they (Kumar *et al.* 2010) have also observed the combined effect of the form drag inertia on the stability of the flow is more intensive when media is highly permeable.

In vertical porous medium pipe, Bera & Kumar (2011) have analyzed least stable mode of buoyancy assisted mixed convective flow using non-Darcy model. They have found that based on media permeability, the flow will be least stable under either first azimuthal mode or zero azimuthal mode.

Few papers are also reported on impact of LTNE state on mixed convective flow in the vertical systems. Ahmed et al. [19] have examined mixed convection in a vertical annular cylinder under LTNE state, whereas, Khandelwal & Bera (2012) have studied a fully developed mixed convection in a vertical channel and have found some significant impact of LTNE parameters on basic state. A double diffusive mixed convection in a vertical pipe under LTNE state is also reported by Bera *et al*. (2012). They have observed a kind of distortion appears on the velocity profile, when buoyancy forces are opposing to each other.

The above literature review indicates that, by using linear stability analysis, the study of mixed convective flow in a vertical annulus filled with porous media under local thermal non-equilibrium condition (LTNE) has not been considered yet. Therefore, an attempt has been made in this direction by investigating the linear stability features of above flow in a vertical annulus.

2. Mathematical Formulation of Physical Problem

A fully developed mixed convective flow caused by an external pressure gradient and a buoyancy force in a vertical annulus filled with porous medium is considered. The inner wall temperature is assumed to vary linearly with z^* as $T_w = T_o + C_1 z^*$, where C_1 is a positive constant and T_o is the upstream reference wall temperature. The inner cylinder is of radius r_i and the outer cylinder is of radius r_0 (shown in Figure 1). The governing equations are written under the assumption of Darcy- Brinkman-Forchheimer model that includes Laplacian term to satisfy the no-slip boundary condition. The Brinkman term is also found to be needed for satisfying a no-slip boundary condition at solid walls, whereas the Forchheimer term due to the form drag. Density is kept constant except in the buoyancy term in the momentum equation, which is satisfied by the Boussinesq approximation. The fluid and solid phases are in local thermal non-equilibrium state i.e. the temperature of fluid and solid phases are defined by different energy equations.

Using non-dimensional quantities:

$\eta = \frac{r^* - r_i}{r_0 - r_i}$, $A = \frac{r_i}{r_0 - r_i}$, $u = \frac{u^*}{W_c^*}$, $v = \frac{v^*}{W_c^*}$, $w = \frac{w^*}{W_c^*}$, $z = \frac{z^*}{r_0 - r_i}$, $p = \frac{p^*}{\rho_f W_c^{*2}}$, $\theta_f = \frac{T_w - T_f^*}{C_1 (r_o - r_i) RePr}$ and $\theta_s = \frac{T_w - T_s^*}{C_1 (r_o - r_i) RePr}$, the non-dimensional governing equations may be written as:

$$\frac{\partial u}{\partial \eta} + \frac{u}{(\eta + A)} + \frac{1}{(\eta + A)} \frac{\partial v}{\partial \psi} + \frac{\partial w}{\partial z} = 0 \quad (1)$$

$$\left[\frac{1}{\epsilon}\frac{\partial u}{\partial t} + \frac{1}{\epsilon^2}\left(Ju - \frac{v^2}{(\eta + A)}\right)\right] + F\left(\sqrt{u^2 + v^2 + w^2}\right)u = -\frac{\partial p}{\partial \eta} + \frac{1}{Re}\left[D^2 u - \frac{2}{(\eta + A)^2}\frac{\partial v}{\partial \psi} - \frac{u}{(\eta + A)^2}\right] - \frac{\Lambda}{ReDa} u \quad (2)$$

$$\left[\frac{1}{\epsilon}\frac{\partial v}{\partial t} + \frac{1}{\epsilon^2}\left(Jv + \frac{uv}{(\eta + A)}\right)\right] + F\left(\sqrt{u^2 + v^2 + w^2}\right)v = -\frac{1}{(\eta + A)}\frac{\partial p}{\partial \psi} + \frac{1}{Re}\left[D^2 v + \frac{2}{(\eta + A)^2}\frac{\partial u}{\partial \psi} - \frac{v}{(\eta + A)^2}\right] - \frac{\Lambda}{ReDa} v \quad (3)$$

$$\left[\frac{1}{\epsilon}\frac{\partial w}{\partial t} + \frac{1}{\epsilon^2}(Jw)\right] + F\left(\sqrt{u^2 + v^2 + w^2}\right)w = -\frac{\partial p}{\partial z} + \frac{1}{Re}[D^2 w] - \frac{\Lambda}{ReDa} w - \frac{Ra}{Re}\theta_f \quad (4)$$

$$RePr\left[\frac{\partial \theta_f}{\partial t} + \frac{1}{\epsilon}(J\theta_f)\right] = \frac{w}{\epsilon} + (D^2 \theta_f) + H(\theta_s - \theta_f) \quad (5)$$

$$RePr\Gamma \frac{\partial \theta_s}{\partial t} = D^2 \theta_s + H\gamma(\theta_f - \theta_s) \quad (6)$$

Where,

$$J = u\frac{\partial}{\partial \eta} + \frac{v}{(\eta + A)}\frac{\partial}{\partial \psi} + w\frac{\partial}{\partial z} \quad \text{and} \quad D^2 = \frac{\partial^2}{\partial \eta^2} + \frac{1}{(\eta + A)}\frac{\partial}{\partial \eta} + \frac{1}{(\eta + A)^2}\frac{\partial^2}{\partial \psi^2} + \frac{\partial^2}{\partial z^2}$$

2.1 Basic Flow

The mean flow, whose stability we wish to analyze is assumed to be steady, unidirectional and fully developed. Therefore, the flow is in vertical direction only i.e. the velocity vector is $(0,0,W_0)$. As a consequence of this, the governing differential equations (1)-(6) for momentum and energy, in cylindrical coordinate, of the basic flow can be written as:

$$\frac{d^2W_0}{d\eta^2}+\frac{1}{\eta+A}\frac{dW_0}{d\eta}-\frac{\Lambda}{Da}W_0-Ra\Theta_f-Re\frac{dp}{dz}-ReF|W_0|W_0=0 \quad (7)$$

$$\frac{d^2\Theta_f}{d\eta^2}+\frac{1}{\eta+A}\frac{d\Theta_f}{d\eta}=\frac{W_0}{\epsilon}+H(\Theta_f-\Theta_s) \quad (8)$$

$$\frac{d^2\Theta_s}{d\eta^2}+\frac{1}{\eta+A}\frac{d\Theta_s}{d\eta}=H\gamma(\Theta_s-\Theta_f) \quad (9)$$

The corresponding boundary conditions are given by:

$$W_0=\Theta_f=\Theta_s=0 \quad at\ \eta=0 \quad (10)$$

$$W_0=\frac{d\Theta_f}{d\eta}=\frac{d\Theta_s}{d\eta}=0 \quad at\ \eta=1 \quad (11)$$

In which

W_0, Θ_f , Θ_s , $Re=\frac{{W_c^*}^2(r_0-r_i)}{\nu}$, $Ra=\frac{g\beta_T C_1(r_0-r_i)^4}{\gamma\alpha_f}$, $Da=\frac{K}{(r_0-r_i)^2}$, $F=\frac{1}{C_F(r_0-r_i)}K^{1/2}$, $H=\frac{h(r_0-r_i)^2}{\varepsilon k_f}$, $\gamma=\frac{\varepsilon k_f}{(1-\varepsilon)k_s}$ and $\Lambda=\frac{\mu_f}{\tilde{\mu}}$ are basic velocity, basic fluid temperature , basic solid temperature, Reynolds number (to predict similar flow patterns in different fluid flow situation), Rayleigh thermal number (which measures the thermal buoyancy force), Darcy number (to measure the permeability of the medium), Forchheimer number (which reflects the strength of inertia due to form drag), inter phase heat transfer coefficient , porosity scaled thermal conductivity ratio and viscosity ratio respectively. The axial pressure gradient can be determined by requirement of global mass conservation (Rogers & Yao 1993):

$$\int_0^1(\eta+A)\,W_0d\eta=\frac{1}{2}(1+2A) \quad (12)$$

2.2 Linear Stability Analysis

The stability of the fully developed mean flow is investigated by decomposing all field variables into a mean flow part and infinitesimal disturbances on mean flow. Using normal mode analysis (Drazin 2004), the solution of the three dimensional problem can be written in the form:

$$(u,v,w,\theta_f,\theta_s,p) = (\tilde{u},\tilde{v},W_0(\eta)+\tilde{w},\Theta_f(\eta)+\tilde{\theta}_f,\Theta_s(\eta)+\tilde{\theta}_s,P_o(z)+\tilde{p}) \quad (13)$$

The tilde quantities denote the infinitesimal disturbances on the corresponding terms and can be represented by

$$(\tilde{u},\tilde{v},\tilde{w},\tilde{\theta}_f,\tilde{\theta}_s,\tilde{p}) = (\hat{u}(\eta),\hat{v}(\eta),\hat{w}(\eta),\hat{\theta}_f(\eta),\hat{\theta}_s(\eta),\hat{p}(\eta))e^{[i\alpha(z-ct)+n\psi]} \quad (14)$$

where α is the wave number and n is integer azimuthal wave number. Here, $c=\hat{c}_r+i\hat{c}_i$ is the complex wave speed. The rate of growth or decay of disturbance is determined by $\hat{c}_i$. The flow is stable, neutrally stable, or unstable accordingly as $\hat{c}_i$ is negative, equal to zero or positive respectively. Following the standard linear stability method, the governing linear equations for the infinitesimal disturbances can be written as:

$$\frac{d\hat{u}}{d\eta}+\frac{\hat{u}}{(\eta+A)}+i\frac{n}{(\eta+A)}\hat{v}+i\alpha\hat{w}=0 \quad (15)$$

$$\frac{d^2\hat{u}}{d\eta^2}+\frac{1}{(\eta+A)}\frac{d\hat{u}}{d\eta}-\left[\frac{1+n^2}{(\eta+A)^2}+\alpha^2+\frac{1}{Da}+i\alpha Re\left(\frac{W_0}{\epsilon^2}-\frac{c}{\epsilon}\right)+ReF|W_0|\right]\hat{u}-\frac{2in}{(\eta+A)^2}\hat{v}-Re\frac{d\hat{p}}{d\eta}=0 \quad (16)$$

$$\frac{d^2\hat{v}}{d\eta^2}+\frac{1}{(\eta+A)}\frac{d\hat{v}}{d\eta}-\left[\frac{1+n^2}{(\eta+A)^2}+\alpha^2+\frac{1}{Da}+i\alpha Re\left(\frac{W_0}{\epsilon^2}-\frac{c}{\epsilon}\right)+ReF|W_0|\right]\hat{v}+\frac{2in}{(\eta+A)^2}\hat{u}-\frac{inRe}{(\eta+A)}\hat{p}=0 \quad (17)$$

$$\frac{d^2\hat{w}}{d\eta^2}+\frac{1}{(\eta+A)}\frac{d\hat{w}}{d\eta}-\left[\frac{n^2}{(\eta+A)^2}+\alpha^2+\frac{1}{Da}+i\alpha Re\left(\frac{W_0}{\epsilon^2}-\frac{c}{\epsilon}\right)+2ReF|W_0|\right]\hat{w}-\frac{1}{\epsilon^2}\frac{dW_0}{d\eta}Re\hat{u}-Ra\hat{\theta}_f-i\alpha Re\hat{p}=0 \quad (18)$$

$$\frac{d^2\hat{\theta}_f}{d\eta^2}+\frac{1}{(\eta+A)}\frac{d\hat{\theta}_f}{d\eta}-\left[\frac{n^2}{(\eta+A)^2}+\alpha^2+H+i\alpha RePr\left(\frac{W_0}{\epsilon}-c\right)\right]\hat{\theta}_f+H\hat{\theta}_s+\frac{\hat{w}}{\epsilon}-\frac{RePr}{\epsilon}\frac{d\Theta_f}{d\eta}\hat{u}=0 \quad (19)$$

$$\frac{d^2\hat{\theta}_s}{d\eta^2}+\frac{1}{(\eta+A)}\frac{d\hat{\theta}_s}{d\eta}-\left[\frac{n^2}{(\eta+A)^2}+\alpha^2+H\gamma-ic\alpha RePr\Gamma\right]\hat{\theta}_s+H\gamma\hat{\theta}_f=0 \quad (20)$$

The required boundary conditions are:

$$\hat{u}=\hat{v}=\hat{w}=\hat{\theta}_f=\hat{\theta}_s=\frac{d\hat{p}}{d\eta}=0 \ at\ \eta=0 \quad (21)$$

$$\hat{u}=\hat{v}=\hat{w}=\frac{d\hat{\theta}_f}{d\eta}=\frac{d\hat{\theta}_s}{d\eta}=\frac{d\hat{p}}{d\eta}=0\ at\ \eta=1 \quad (22)$$

The above equations (15-20) along with boundary conditions (21-22) are solved numerically by using the spectral Chebyshev collocation method. The details of this method and implementation can be seen in ([20, 21]).

3. Results and Discussion

Linear stability analysis of mixed convective flow has been attempted here to understand the cause for the occurrence of the maximum stability of fluid flow in a vertical annulus filled with porous media under LTNE state. A wide range of controlling parameters of thermal non-equilibrium state has been considered. Here, we focus on the impact of LTNE parameters: H, γ on instability boundary of different fluids, covering different range ($[10^{-3}, 10]$) of Prandtl number (*Pr*). In this study, we have considered two discrete values $(10^{-1}, 10^{-2})$ of Da and porosity at 0.97. We have also fixed the curvature parameter (A) at 0.6 as from mean flow study (Bhowmik & Bera 2013), it is observed that beyond this value, the impact of *A* is almost negligible. The dependence of the stability boundaries on azimuthal wave numbers n (= 1, 2, 3, 4) is plotted in (*Pr*, *Ra*) plane, for three different values (1, 10, 100) of *H* and three different values $(10^{-3}, 10^{-2}, 10^{-1})$ of γ. Before discussing the effect of different controlling parameters on the instability boundaries, we have verified our numerical results presented in this paper by comparing with published results (Rogers & Yao 1993) in viscous media. For viscous media case (taking $Da = 10^{10}, \epsilon = 1, H = 0, F = 0, Re = 250$) the solution generated by this code is very close to Rogers et al. results (see Table 1). This is an excellent agreement with published one. We have also checked grid independence test under local thermal non-equilibrium state, the results remain consistent on consideration of order of polynomial as beyond 50 in Chebyshev approximations. In this study we have considered 50 order Chebyshev polynomial.

3.1 Description of Basic Flow

Before analyze the linear stability, we have investigated the influence of local thermal non-equilibrium parameters (H and γ), on the basic velocity profiles, which is shown in Figure 2. This figure is plotted for different values of H and γ at *Ra* = 1000 and $Da = 10^{-1}$. It can be observed from above figure, at γ =0.001 and *H* < 25 the velocity profiles contain point of inflection, which is died out for large value of *H* (> 25). Similarly, we can also seen that on increasing the value of γ, the velocity profiles possess point of inflection. Similar types of results are also observed for $Da = 10^{-2}$ (figure not shown here). The appearance of point of inflection on the velocity profile may lead the instability of the basic flow for buoyancy assisted case which is given in (Rogers *et al*. 1993). Hence, increasing *H* makes the flow profile smooth and stabilizes the flow in the annulus, whereas, γ destabilized it.

3.2 Instability Mechanism

In this subsection the critical value of Ra and α is denoted by Ra and α. The dependence of the stability boundaries on the azimuthal wave numbers (*n* = 0, 1, 2, 3, 4) for different values of *H* and γ is plotted in (*Pr*, Ra) plane. In this analysis, *Re* and *F* are fixed at 500 and 0.001 respectively. Figure 3(a)-3(c) is plotted for $Da = 10^{-1}$. It is observed that, for *H* = 1 the zero azimuthal mode (*n* = 0) is the least stable mode for all considered values of γ in the entire domain of *Pr* (see Figure 3(a)). But in case of *H* = 10, depending on *Pr* the least stable mode may be zero or first azimuthal number. For $Pr \leq 1$, the least stable mode is first azimuthal mode beyond that zero azimuthal mode is the least stable mode for all values of γ (see Figure 3(b)) Again if we increase the value of *H* from 10 to 100, the least stable is also characterized by γ, which can be seen from Figure 3(c). It is observed that for γ = 0.001, *n* = 3 is the least stable mode for $Pr < 0.5$ otherwise zero azimuthal mode becomes least stable. As the value of γ is replaced by 0.01, *n* = 2 and *n* = 0 are least stable mode in the ranges [0, 2) and [2, 10] of *Pr* respectively. But for the same value of *H*, if the value of γ is fixed at 0.1, first azimuthal mode is the least stable mode for *Pr* < 3. Of course, both curves (obtained for *n* = 0, 1) almost coincide each other and beyond that, *n* = 0 is the least stable mode. Figure 4(a)-4(c) is plotted for relatively low permeable media ($Da = 10^{-2}$) for different values of H and γ. As can be seen from this figure, the first azimuthal mode is the least stable mode in the domain [0, 0.5] of *Pr*, beyond that zero is always the least stable mode for all considered values of H and γ. In the above analysis we have seen that the impact of the thermal non-equilibrium is much more significant in the high permeable media. The impact of γ on stability boundaries is independent for relatively small value of *H* but it has significant impact on it for large value of *H*.

The following observations can also be carried out from above figures. First, on increasing the value of *H* increases the value of the critical *Ra*, whereas increase in γ decreases the value of the critical *Ra*. This shows that *H* stabilizes the basic flow, whereas γ destabilizes it. The qualitative explanation for the physics involved behind the above observation is, when all other parameters are fixed, on changing *H* from lower to higher value increases the volumetric inter-phase heat transfer coefficient, which in turn, increases the heat transfer rate of the solid. The corresponding heat transfer rate of fluid is also increased for a certain value of *H*, which is function of *Da*. Releasing more heat from the system annihilates the thermal fluctuation due to disturbances, which in turn, makes the system more stable. Second, the critical value of *Ra* decreases on increasing the value of *Pr* for all three values of γ as well as *H*, i.e. increase in *Pr* destabilizes the basic flow. Third, irrespective of the fluid, the base flow is more stable for relatively low permeable media.

In order to understand the same in detail, a quantitative analysis is presented here. If we change *Da* from 10^{-2} to 10^{-1}, while the other parameters H, γ and Pr are fixed at 10, 0.01 and 7 respectively, the corresponding critical Ra is reduced from 899.72 to 615.47. This indicates that in low permeable media the flow is more stable compare to high permeable media. In contrast to purely viscous fluid flow (Rogers & Yao 1993) in which first azimuthal mode is the least stable mode, in porous media, zero azimuthal mode is least stable mode for fluid like water ($Pr = 7$). As a result, two azimuthal modes: $n = 0$ and 1 are used to find the least stable mode of the basic flow. By Figures 3 and Figure 4 it is clear that, a higher Prandtl number is associated with a lower critical Rayleigh number, that is, the effect of Prandtl number is destabilizing. For example in case of air ($Pr = 0.7$), $Da = 10^{-1}$, $\gamma = 0.01$ and $Re = 500$, on one order enhancement of H (i.e. by changing H from 1 to 10) critical value of Ra is changed from 727 to 2109, i.e., the basic flow will be 3 times more stable. At the same time, as H is increased further one order, by changing it from 10 to 100, the corresponding Ra is changed from 2109 to 43995, i.e. basic flow remains stable 20.8 times than the same at $H = 10$. However, when Pr is replaced by 7 i.e. for water, the corresponding critical Ra is changed as 148 to 615 and 615 to 6411 on the stepwise changing of H from 1 to 10 and 10 to 100 respectively. This shows that the stability of the flow increases 4.2 times, on changing H from 1 to 10, and 10.4 times on changing the same from 10 to 100. This indicates that impact of H on stabilizing the flow is much significant for small values of Pr. Finally, observation regarding impact of γ on flow stability shows that for relatively small values of H impact of such change on thermal conductivity will not be much effective. But for high values of H, impact of γ is expected. For example, when H and Pr are fixed at 100 and 7 respectively, a stepwise increase of γ from 0.001 to 0.01 and from 0.01 to 0.1, change the critical Ra from 9003 to 6411, and 6411 to 3144, respectively. However, for $H = 1$, the same remains as 148 and is independent of γ.

4. Conclusion

We have attempted a linear stability of mixed convective flow in a vertical annulus filled with fluid-saturated porous media. In the entire study, we have adopted Non-Darcy Brinkman-extended model. The fluid and solid phases are in local thermal non-equilibrium state. The governing equations together with the Spectral collocation method have been used to study the linear stability of the basic flow. By means of linear theory, we are able to extract detailed information of the stability of the basic flow through a porous medium for different fluids. The main objective in this study is to investigate the dependence of the stability boundaries on the azimuthal wave numbers (n) for LTNE parameters (H, γ). In this study, we have found that depending on the values of media permeability as well as Prandlt number, the flow will be least stable under either first azimuthal mode or zero azimuthal mode. It is also found that enhancement of Prandtl number (Pr) destabilize the basic flow. Although the fully developed flow is free from Pr but the present study discloses that, in stability characteristic, it plays a vital role. The stability analysis also indicates that enhancement of media permeability destabilizes the basic flow. Apart from this on increasing the interphase heat transfer coefficient, in terms of increasing H, increases stability of the basic flow/mean flow, whereas, decreasing conductivity of the solid porous matrix, in terms of increasing porosity scaled conductivity ratio (γ), reduces the flow stability for relatively large value of H. In nutshell, H stabilizes the flow, whereas γ destabilizes it.

References

Ahmed, N.J.S., Badruddin, I.A., Kanesan, J., Zainal, Z.A., Ahamed, K.S.N. (2011), "Study of Mixed Convection in an Annular Vertical Cylinder Filled with Saturated Porous Medium, Using Thermal Non-equilibrium Model", *International Journal of Heat and Mass Transfer* 54, 3822-3825.

Bera, P., Khalili, A. (2002), "Stability of Mixed Convection in an Anisotropic Porous Channel", *Physics of Fluids* 14, 1617-1630.

Bera, P., Khalili, A. (2006), "Influence of Prandtl Number on Stability of Mixed Convective Flow in a Vertical Channel Filled with a Porous Medium", *Physics of Fluids* 18, 124103-124110.

Bera, P., Khalili, A. (2007), "Stability of Buoyancy Opposed Mixed Convection in a Vertical Channel and its Dependency on Permeability", *Advances in Water Resources* 30, 2296-2308.

Bera, P., Kapoor, S., Khandelwal, M.K. (2012), "Double- Diffusive Mixed Convection in a Vertical
Pipe: a Thermal Non-equilibrium Approach", *International Journal of Heat and Mass Transfer* 55, 7079-7092.

Bera, P., Kumar, A. (2011), "Analysis of Least Stable Mode of Buoyancy Assisted Mixed Convective Flow in Vertical Pipe Filled with Porous Medium", *Proceedings Conference of World Congress on Engineering*, London, 70 .

Bhowmik , M., Bera, P. (2013), "A Thermal Non-equilibrium Approach on Non-Darcy Mixed Convective Flow in a Vertical Annulus", *Proceedings Conference of the 22nd National and 11th International ISHMT-ASME Heat and Mass Transfer, India*, 488.

Calmidi, V.V., Mahajan, R.L. (2000), "Forced Convection in High Porosity Foams", *Transaction of the ASME Journal of Heat Transfer* 122, 557-565.

Chen, Y. C., Chung, J. N. (1996), "The Linear Stability of Mixed Convection in a Vertical Channel", *Journal of Fluid Mechanics* 325, 29-51.
Chen, Y.C. (2004), "Non-Darcy Flow Stability of Mixed Convection in a Vertical Channel Filled with a Porous Medium", *International Journal of Heat and Mass Transfer* 47, 1257-1266.
Drazin, P.G., Reid, W.H. (2004), "Hydrodynamic Stability", *Cambridge University Press*, Cambridge.
Kumar, J., Bera, P., Khalili, A. (2010), "Influence of Inertia and Drag Terms on the Stability of Mixed Convection in a Vertical Porous Medium Channel", *International Journal of Heat and Mass Transfer* 53, 5261-5273.
Khandelwal, M.K., Bera, P. (2012), "A Thermal Non-equilibrium Perspective on Mixed Convection in a Vertical Channel", *International Journal of Thermal Science*. 56, 23-34.
Nield, D.A., Bejan, A. (2013), "Convection in Porous Media", *4th ed., Springer-Verlag*, NewYork.
Rao, D. V., EL-GENK, M. S. (1990), " Buoyancy Induced Instability of Laminar Flows in Vertical Annuli-II Model Development and Analysis", *International Journal of Heat and Mass Transfer* 33, 2145-2159.
Vafai, K. (2005), "Handbook of Porous Media", *2nd ed., Taylor and Francis,* New York.
Rogers, B. B., Yao, L. S. (1993), " The Importance of Prandtl Number in a Mixed Convection Instability", *Journal of Heat Transfer* 115, 482-486.
Rogers, B.B., Moulic, S.G., Yao, L.S. 1993, "Finite-amplitude Instability of Mixed Convection", *Journal of Fluid Mechanics,* 254, 229-250.
Su, Y.C., Chung, J.N. (2000), "Linear Stability Analysis of Mixed Convection Flow in a Vertical Pipe", *Journal of Fluid Mechanics* 422, 141-166.
Yao, L.S. (1987a), "Is a Fully-developed and Non-isothermal Flow Possible in a Vertical Pipe?", *International Journal of Heat and Mass Transfer* 30, 707 -716.
Yao, L.S. (1987b), "Linear Stability Analysis for Opposed Mixed Convection in a Vertical Pipe", *International Journal of Heat and Mass Transfer* 30, 810-811.
Yao, L. S., Rogers, B. B. (1989a), "The Linear Stability of Mixed Convection in a Vertical Annulus", *Journal of Fluid Mechanics* 201, 279-298.
Yao, L. S., Rogers, B. B. (1989b), "Mixed Convection in an Annulus of Large Aspect Ratio", *ASME Journal of Heat Transfer* 111, 683-689.
Zorrilla, S.E., Rubiolo, A.C. (2005), "Mathematical Modeling for Immersion Chilling and Freezing of Foods", *Part I. Model development, J. Food Engineering* 66, 329-338.

Acknowledgments
One of the authors, Moumita Bhowmik, is grateful to MHRD India for providing financial support during the preparation of this manuscript.

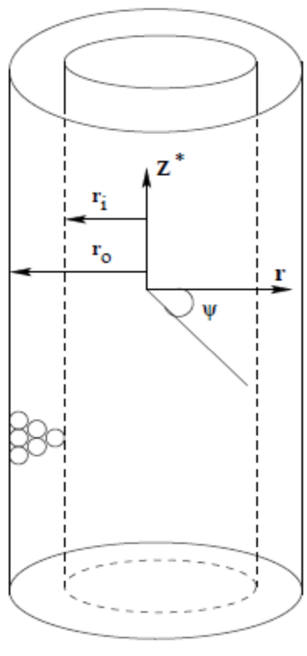

Figure 1. Physical problem and coordinate system.

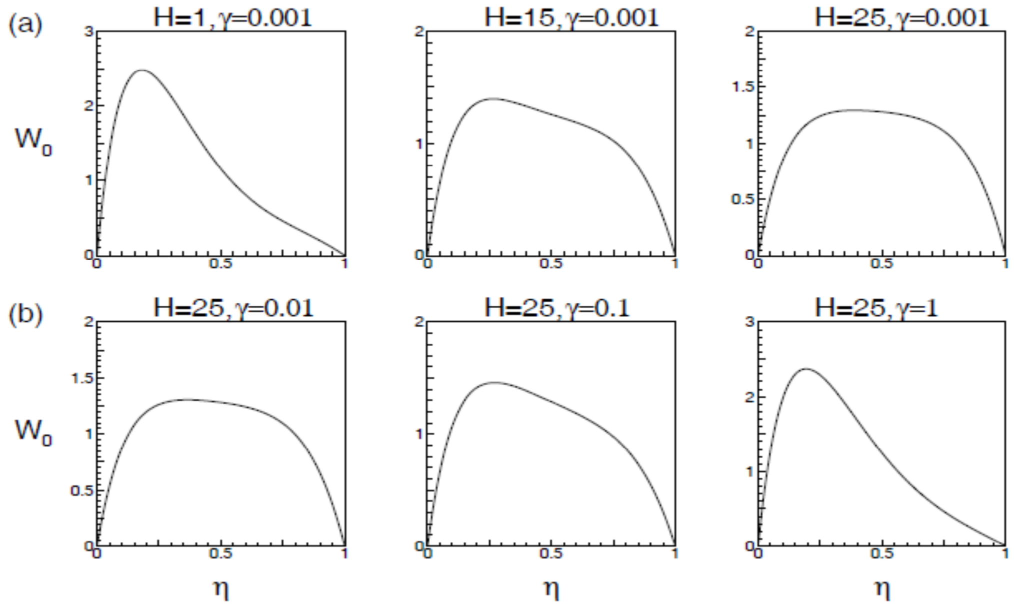

Figure 2. Velocity profiles of flow for specific values of H and γ at $Da = 10^{-1}, Ra = 1000$, A = 0.6 and F = 0.001.

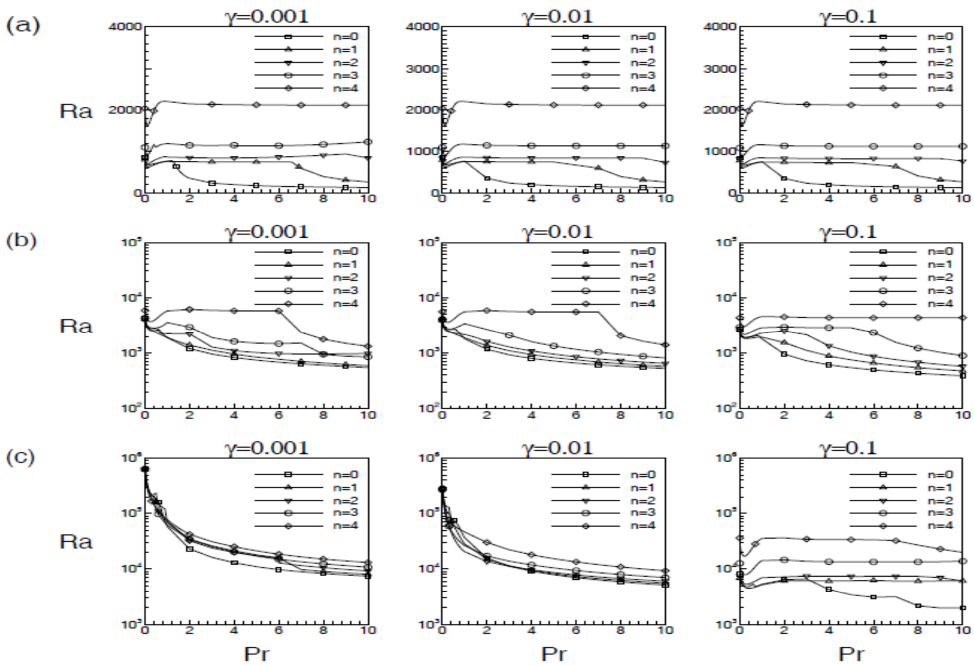

Figure 3. Effect of azimuthal wave number (n) on the stability map of assisted flow for $Da = 10^{-1}$ at (a) H = 1 (b) H = 10 and (c) H = 100.

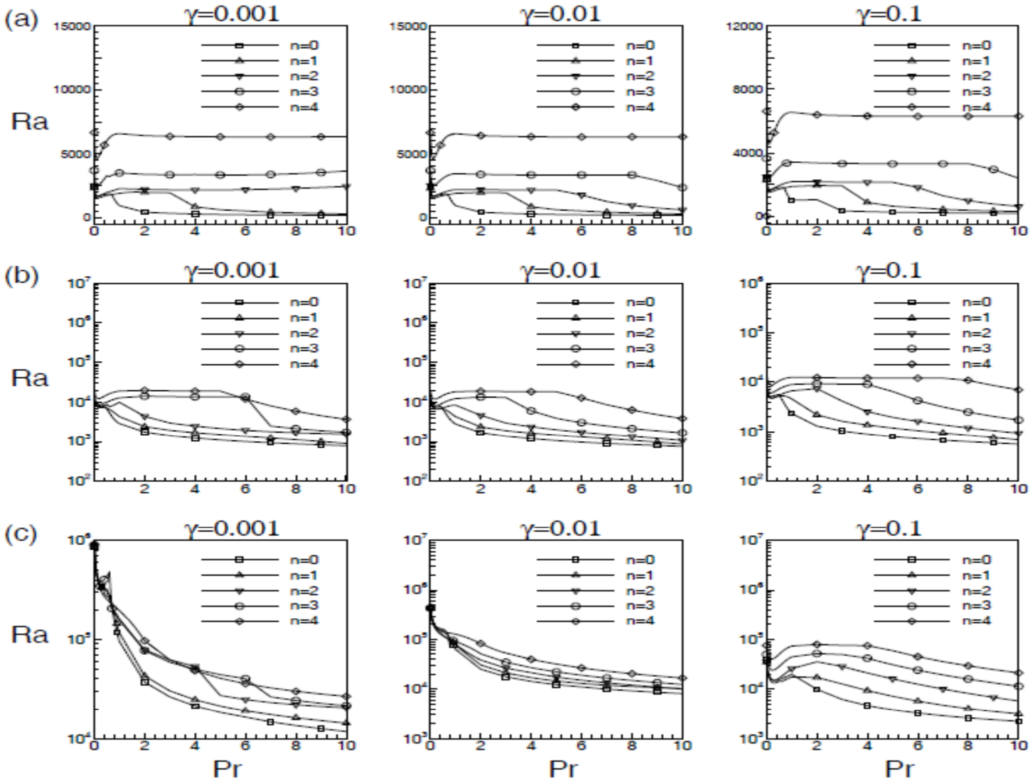

Figure 4. Effect of azimuthal wave number (n) on the stability map of assisted flow for $Da = 10^{-2}$ at (a) $H = 1$ (b) $H = 10$ and (c) $H = 100$.

Table 1. Comparison between published results (Rogers & Yao 1993) and present result ($Da = 10^{10}, H = 0, F = 0, Re = 250, A = 0.6, \epsilon = 1$)

Pr	n	Rogers & Yao (1993)			(Present Study)		
		Ra	α	$\hat{c}_r$	Ra	α	$\hat{c}_r$
0.01	1	219	1.22	1.10	221.524	1.19	1.11
1	1	240	1.16	1.18	239.617	1.15	1.18
6	0	89	0.26	1.65	89.144	0.25	1.65
100	0	33	0.18	1.23	33.890	0.17	1.23